Mode reconstruction of a light field by multiphoton statistics

Elizabeth A. Goldschmidt,[1,2,*] Fabrizio Piacentini,[3] Ivano Ruo Berchera,[3] Sergey V. Polyakov,[2] Silke Peters,[4] Stefan Kück,[4] Giorgio Brida,[3] Ivo P. Degiovanni,[3] Alan Migdall,[1,2] and Marco Genovese[3]

[1]*Joint Quantum Institute, University of Maryland, College Park, Maryland 20742, USA*

[2]*National Institute of Standards and Technology, 100 Bureau Drive, Gaithersburg, Maryland 20899, USA*

[3]*Istituto Nazionale di Ricerca Metrologica INRIM, Strada delle Cacce 91, 10135 Torino, Italy*

[4]*Physikalisch-Technische Bundesanstalt Braunschweig, Bundesallee 100, 38116 Braunschweig, Germany*

(Received 31 January 2013; published 15 July 2013)

We present a simple method to reconstruct the mode distribution of multimode classical and nonclassical optical fields using a single measurement of higher-order photon number correlation functions. Knowing the underlying number and structure of occupied modes of a light field plays a crucial role in minimizing loss and decoherence of quantum information. Typically, full characterization of the mode structure involves a series of several separate measurements in spatial, temporal, frequency, and polarization domains. We experimentally demonstrate reconstruction of up to three modes with excellent agreement and study the robustness of our method in experimentally realizable regimes.

DOI: 10.1103/PhysRevA.88.013822 PACS number(s): 42.50.Ar, 03.65.Wj, 42.50.Dv

I. INTRODUCTION

Characterizing the underlying processes contributing to a light field has wide ranging applications throughout physics. For instance, knowledge of the mode structure is vital for engineering sources of nonclassical light that minimize loss and decoherence of quantum information due to coupling to unwanted modes. Such applications include mode-matching biphoton collection [1], producing factorizable states of photon pairs [2], minimizing classical background emission from single-emitter sources [3], and characterizing the number and degree of squeezing in multimode continuous variable entangled states [1,4–8].

Photon-number statistics are used to characterize a variety of optical systems including single-photon sources [9–11], photon pair sources [12–14], cavity QED [15,16], and lasers [17,18]. In most cases, these measurements have been limited to single- and twofold photodetection, or first- and second-order optical coherence. In terms of understanding the underlying processes contributing to the light field, this can provide only limited information, such as a measure of the purity of the system. Recent developments in photon-number resolving (PNR) detectors [19–21] allow simpler measurement of higher-order correlations, and such measurements should continue to become more routine [22–24]. We show that this additional information can allow a full characterization of the various quantum and classical modes present in a light field. We present and implement experimentally a method to reconstruct the underlying mode structure of an optical field using high-order photon-number statistics.

Typically, full characterization of the mode structure involves a series of separate measurements in spatial, temporal, frequency, and polarization domains, requiring a range of instrumentation. However, our method can be easily integrated into existing optical systems as it uses only a single measurement of the photon-number distribution of a field. Also, full mode reconstruction allows a more subtle distinction between classical and nonclassical fields. We show how a full reconstruction of the underlying mode structure of a field can provide information about nonclassical components of a nominally classical field. We consider multimode light from a single source, such as multimode thermal light from spontaneous parametric down conversion (SPDC), as well as from multiple sources, each producing light in one or more modes, such as attenuated single photons from a single emitter and coherent light from a laser. We note, however, that this method is extremely general and can be used for any combination of sources, though only the total fraction of the power with underlying Poissonian statistics can be determined. We perform a proof of principle experiment using PNR detection and mixed states with contributions from one or more modes with thermal statistics, up to one mode with attenuated single-photon statistics, and up to one mode with Poissonian statistics. We successfully identify the distribution of contributions from up to three total modes of classical and nonclassical light. We also theoretically study the robustness and prospects of our method in experimentally accessible regimes.

II. METHOD

It is straightforward to write down the full photon-number probability distribution for a given mode structure with mean photon numbers μ_i in the modes. For thermal and Poissonian statistics $\mu = \langle n \rangle$ is the mean photon number and for attenuated single-photon statistics μ is the probability of finding a single photon. The photon-number probability distribution is uniquely described by a probability generating function $G(s)$, which is the product of the generating functions for all the underlying modes where $G_{\text{thermal}}(s) = [1 + \mu(1-s)]^{-1}$, $G_{\text{single photon}}(s) = [1 - \mu(1-s)]$, and $G_{\text{Poissonian}}(s) = e^{-\mu(1-s)}$ [25]. It is convenient to translate this into a set of relations between the μ_i and the intensity autocorrelation functions (at zero time difference), $g^{(k)}(0) = g^{(k)} = \langle :\hat{n}^k: \rangle / \langle \hat{n} \rangle^k$, where $\langle :: \rangle$ denotes normal ordering of the operators. We find that $g^{(k)} = G^{(k)}(s=1)/(\mu_{\text{total}})^k$, where

*egolds@nist.gov

$G^{(k)}(s=1)$ is the kth derivative of $G(s)$ evaluated at $s=1$. Clearly $g^{(1)}$ is always unity, so the first-order expression we use is $\langle n\rangle = \mu_{\text{total}} = \sum \mu_i$. We use this set of nonlinear relations to find the full mode distribution in the form of a set of μ_i. It is straightforward to demonstrate that for the mixed states considered here, N orders of correlation functions are required to fully determine the mode occupation for light with contributions from N modes. For $\mu_{\text{total}} \ll k$, photon-number resolution up to k photons is required to accurately measure $g^{(k)}$. Overdetermining the system, by using more than N correlation functions to reconstruct N modes, can improve the accuracy of reconstruction. It is important to note that we must guess what types of modes could be contributing to the field, though we see below that there is no penalty for assuming potential modes that are not in fact present.

As an example, we consider a field that is a mixed state with contributions from one thermal mode, one single-photon mode, and one Poissonian mode and a fixed μ_{total}. By varying the fraction of power contributed by each mode, such a mixed state can exhibit $g^{(2)}$ between zero (all single photon) and 2 (all thermal). For any $g^{(2)}$ between these extremes, there is a family of possible mode distributions. Figure 1(a) shows curves of constant $g^{(2)}$, $g^{(3)}$, and $g^{(4)}$ as a function of the fraction from Poissonian and single-photon modes. The bold $g^{(2)}$ curve is $g^{(2)}=1$, which includes the extreme cases of Poissonian light only and an equal mixture of thermal and single-photon light. For two particular mode distributions between those extremes (points 1 and 2) lines of constant $g^{(3)}$ and $g^{(4)}$ are plotted. We see that although $g^{(2)}$ is identical, the higher-order correlation functions are not, demonstrating how a three-mode distribution can be uniquely identified by μ_{total} plus two orders of the correlation function.

We plot the correlation function contours that intersect at two additional points for reference. The inset is the mode structure at the four points noted on the main plot. $g^{(2)}=1$ is typically thought of as the border between classical (unshaded) and nonclassical (shaded) fields. However, all configurations here have some contribution from an explicitly nonclassical mode (single photons). Only by reconstructing the full mode structure can we see the nonclassical component of a field with $g^{(2)}>1$ (see point 4).

We noted above that a set of N correlations is required to uniquely describe a set of N modes; however, including additional orders of correlations will further distinguish different sets of modes. We study the expected improvement gained by using higher-order correlations in terms of the sensitivity of the photon-number distribution to the mode structure. The particular figure of merit we consider is a function of the gradients of the correlation functions, $\sum_k (\nabla_{\vec{\mu}} g^{(k)}[\vec{\mu}]/g^{(k)}[\vec{\mu}])^2$, where $\vec{\mu}$ is the set of μ_i. In Fig. 1(b) we show the ratio of this quantity with six modes included compared to only three modes. We see a gain in sensitivity for all mode configurations and the gain is largest near the fully Poissonian configuration. We note that this is the configuration where the photon-number statistics are least sensitive to the mode structure because all orders of the correlation function are near unity. Higher-order photon-number resolution, up to ten photons or more, is becoming possible with new PNR detectors. With such detectors, one can trade off including additional modes in the reconstruction for increasing the fidelity of reconstruction.

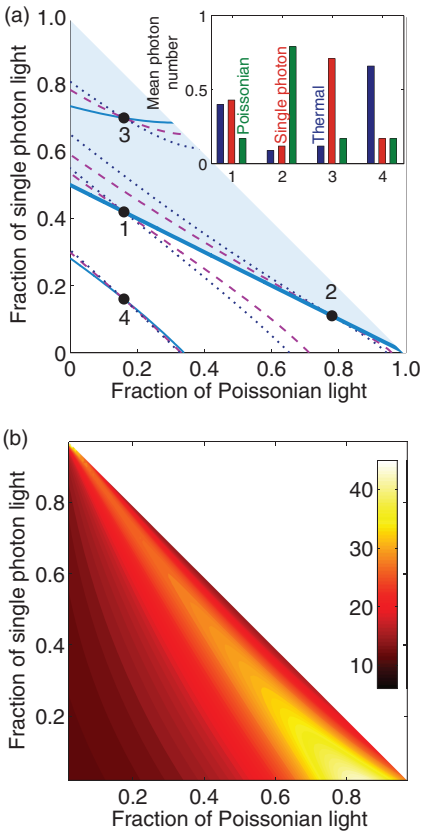

FIG. 1. (Color online) Example case of one thermal mode, one single-photon mode, one Poissonian mode, and fixed μ_{total}. (a) Lines of constant $g^{(2)}$ (solid blue), $g^{(3)}$ (dashed purple), and $g^{(4)}$ (dotted dark blue) plotted against fractions of Poissonian and single-photon light. Bold line is $g^{(2)}=1$ and shaded area represents nominally nonclassical region ($g^{(2)}<1$). Contour line values through point 1: $g^{(2)}=1.0$, $g^{(3)}=1.2$, $g^{(4)}=2.2$; point 2: $g^{(2)}=1.0$, $g^{(3)}=1.0$, $g^{(4)}=1.0$; point 3: $g^{(2)}=0.5$, $g^{(3)}=0.3$, $g^{(4)}=0.2$; point 4: $g^{(2)}=1.4$, $g^{(3)}=2.9$, $g^{(4)}=8.0$. Inset is the mode structure of the four points. Bar heights are the mean photon numbers μ in the thermal mode (left, blue), single-photon mode (middle, red), and Poissonian mode (right, green). (b) Sensitivity gained by using an overdetermined set of six correlation functions compared to three. Color represents the ratio of the gradients for six- to threefold detection at each point in the space.

III. EXPERIMENT

Figure 2 shows the three light sources and the PNR detection scheme that we employ for our experimental demonstration. We generate pseudothermal light by sending a pulsed laser through a rotating ground glass disk. The random phase and amplitude perturbations imparted on the coherent light by the disk produce an incoherent field that approximates a thermally distributed field [26,27]. We find our pseudothermal state has $g^{(2)}>1.9$ in all cases, signifying that we are close to a true thermal state ($g^{(2)}=2$). We use attenuated light directly from the laser for our Poissonian distributed field. And we obtain single photons from a low-noise single-photon source based on SPDC in a periodically poled lithium niobate crystal [28]. In SPDC, photons are always produced in pairs (signal and idler), so detection of one photon heralds the presence

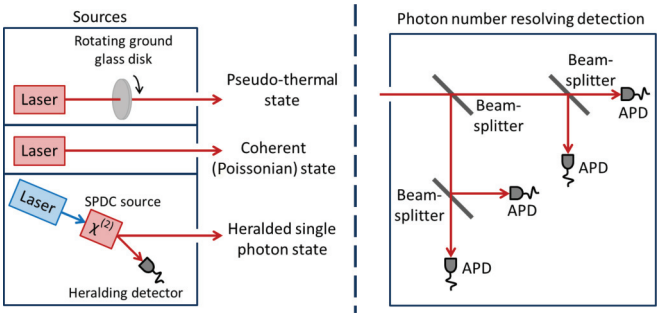

FIG. 2. (Color online) Source and detector configurations. SPDC: spontaneous parametric down conversion. APD: avalanche photodiode.

of the other. Thus the state of the idler field, conditioned on detection of a signal photon, is close to a single-photon Fock state, with $g^{(2)} < 0.05$ in our case [28].

We combine up to three pulsed modes of such light using beam splitters and insert short-time delays between the fields to avoid coherent interference between them. We detect the resulting field with four single-photon avalanche diodes in a tree configuration, providing photon-number resolution up to four photons. We perform appropriate postprocessing of the data according to the positive-operator valued measure of the detection system to obtain the real photon-number distribution [29]. We perform a minimization to find the mode distribution that best fits the measured photon-number statistics.

We use a pulsed source with pulse length much shorter than the coherence time of the pseudothermal light to ensure that the detection window is within the temporal width of the photon bunching [27]. For applications such as SPDC, pulsed excitation, common for such sources, ensures correct measurement of the zero-time correlation functions [30]. In addition, we point out that our method can reconstruct all modes within the broad spectral range of the detector and can reconstruct spectral modes with arbitrarily small frequency difference. Finally, we note that our reconstruction requires only a single measurement of the photon-number distribution of the field, unlike most quantum tomography procedures, which require measurements in multiple configurations to reconstruct the unknown quantum state [31].

We take data in a variety of regimes. First, we detect fields containing one, two, and three thermal modes. In all cases we use the data to reconstruct the detected photon numbers in three thermal modes. Figure 3 shows examples of these fits for one, two, and three incident thermal modes. We find excellent agreement for a range of powers and the reconstruction correctly identifies the actual number of modes present.

Reconstructing a set of modes with underlying thermal statistics is useful for applications involving photon pair sources with such statistics, such as SPDC-based sources. In particular, there are applications which require performing a Schmidt decomposition of such a source [2,32,33] or ensuring the overlap of collected pairwise modes from a highly multimode source [1]. Our method, if applied to the pairwise statistics of such a source, would reconstruct the distribution of pairwise modes without the need to measure the spectral or spatial distribution of the pairs. The extension of this method to pairwise statistics is, however, beyond the scope of this paper.

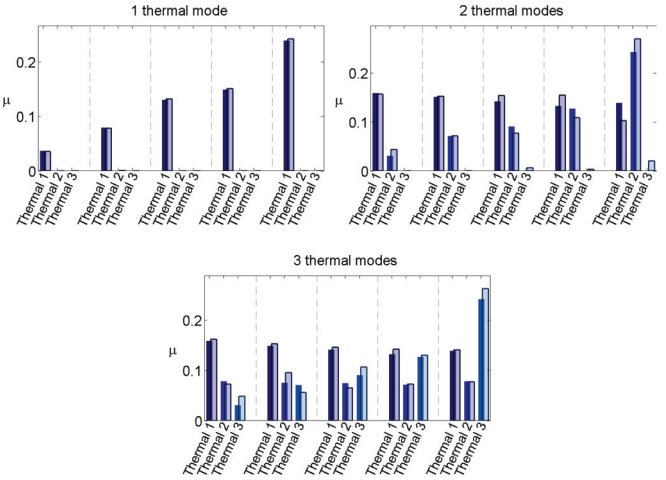

FIG. 3. (Color online) Bar heights are mean photon numbers μ. Each group of three bars represents a single experiment with a particular set of mean photon numbers. Dark bars in back are measured mean photon numbers, $\vec{\mu}_{\mathrm{m}}$, and translucent bars overlaid are the reconstructed mean photon numbers, $\vec{\mu}_{\mathrm{r}}$. Noted above each plot is the set of input modes.

We next take data with zero, one, and two thermal modes plus one Poissonian mode and fit it to two thermal modes plus one Poissonian mode. We fit data with two thermal modes only to two thermal modes plus one Poissonian mode. In Fig. 4, we see excellent agreement for a range of input powers and correctly identify when only one of type of mode (Poissonian or thermal) is present.

Many sources of nonclassical light for quantum information applications, such as SPDC or four-wave mixing, produce single- or multimode light with thermal statistics. In these cases it is important to ensure the desired state is not polluted by laser light, which has Poissonian statistics. Our method

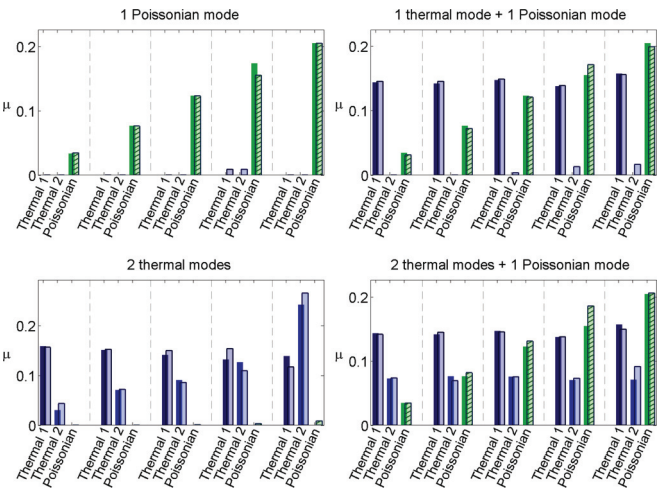

FIG. 4. (Color online) Bar heights are mean photon numbers μ. Each group of three bars represents a single experiment with a particular set of mean photon numbers. Dark bars in back are measured mean photon numbers, $\vec{\mu}_{\mathrm{m}}$, and translucent bars overlaid are the reconstructed mean photon numbers, $\vec{\mu}_{\mathrm{r}}$. Blue bars are thermal modes and rightmost, green, crosshatched bar is Poissonian mode. Noted above each plot is the set of input modes.

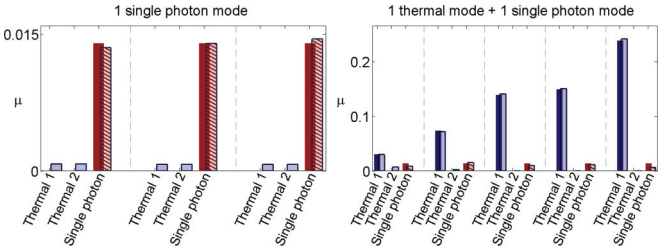

FIG. 5. (Color online) Bar heights are mean photon numbers μ. Each group of three bars represents a single experiment with a particular set of mean photon numbers. Dark bars in back are measured mean photon numbers, $\vec{\mu}_{\mathrm{m}}$, and translucent bars overlaid are the reconstructed mean photon numbers, $\vec{\mu}_{\mathrm{r}}$. Blue bars are thermal modes and rightmost, red, crosshatched bar is single-photon mode. Noted above each plot is the set of input modes.

identifies how much laser pollution is present, even at the same frequency as the thermal light.

Finally, we take data for the heralded single-photon source described above. We fit the data to two thermal modes plus one single-photon mode. We also combine the single-photon data with data for a single thermal mode and fit it to two thermal modes plus one single-photon mode. In Fig. 5 we again find excellent agreement for a range of input powers and our method identifies how many modes and which type of mode are present.

In the second case in Fig. 5, the nonclassical source is heavily polluted with classical thermal light. The mixing of nonclassical and thermal light is common to heralded single-photon sources such as those based on SPDC, because the unheralded statistics are thermal. All the states of mixed classical and nonclassical light are in the nominally classical regime ($g^{(2)} > 1$). However, our method is robust enough to identify the presence of the nonclassical component, whether or not there is a strong classical component present.

We define a fidelity of reconstruction as $f = [2|\vec{\mu}_{\mathrm{m}} \cdot \vec{\mu}_{\mathrm{r}}|/(|\vec{\mu}_{\mathrm{m}}|^2 + |\vec{\mu}_{\mathrm{r}}|^2)]^{1/2}$, where $\vec{\mu}_{\mathrm{m}}$ and $\vec{\mu}_{\mathrm{r}}$ are the sets of measured and reconstructed mean photon numbers, respectively. For all configurations shown, other than the lowest power combination of thermal and single-photon light, the fidelity of reconstruction is greater than 0.99, demonstrating faithful reconstruction for a broad set of input powers and mode configurations. Our method clearly recognizes cases where only one or two modes are present as well as faithfully reconstructing all modes present. We obtain substantially more information than is contained in the second-order correlation function alone, particularly in the cases where we allow the reconstruction to determine the occupation of modes with different statistics. With additional detectors, or a true PNR detector, we should be able to reconstruct more modes, and do so more faithfully.

IV. CONCLUSION

In conclusion, we propose and implement a method to reconstruct the underlying mode structure of multimode classical and nonclassical light fields using detected photon-number statistics. Such reconstructions are vital for engineering and understanding sources that produce light suitable for a wide variety of quantum and classical applications. Our method uses PNR detection to reconstruct the number and structure of occupied modes in all degrees of freedom, with a measurement in a single configuration and without specialized equipment to make separate measurements in the spatial, spectral, polarization, temporal, and other domains. We experimentally demonstrate successful reconstruction of up to three modes and present numerical simulations suggesting the robustness of our method in experimentally realizable regimes.

ACKNOWLEDGMENTS

The research leading to these results has received funding by MIUR, FIRB RBFR10UAUV, by Fondazione San Paolo, by Nato Grant No. 984397, and EMRP (project IND06-MIQC). The EMRP is jointly funded by the EMRP participating countries within EURAMET and the European Union. The authors also acknowledge support from the Physics Frontier Center at the Joint Quantum Institute. The authors thank Stephen Maxwell for fruitful discussions.

[1] G. Brida, M. Genovese, and I. Ruo Berchera, Nat. Photon. **4**, 227 (2010).
[2] W. Mauerer, M. Avenhaus, W. Helwig, and C. Silberhorn, Phys. Rev. A **80**, 053815 (2009).
[3] E. B. Flagg, S. V. Polyakov, T. Thomay, and G. S. Solomon, Phys. Rev. Lett. **109**, 163601 (2012).
[4] V. Boyer, A. M. Marino, R. C. Pooser, and P. D. Lett, Science **321**, 544 (2008).
[5] C. R. Müller, B. Stoklasa, C. Peuntinger, C. Gabriel, J. Řeháček, Z. Hradil, A. B. Klimov, G. Leuchs, C. Marquardt, and L. L. Sánchez-Soto, New J. Phys. **14**, 085002 (2012).
[6] G. Brida, L. Caspani, A. Gatti, M. Genovese, A. Meda, and I. R. Berchera, Phys. Rev. Lett. **102**, 213602 (2009).
[7] A. I. Lvovsky and M. G. Raymer, Rev. Mod. Phys. **81**, 299 (2009).
[8] B. Kanseri, T. Iskhakov, I. Agafonov, M. Chekhova, and G. Leuchs, Phys. Rev. A **85**, 022126 (2012).
[9] C. Kurtsiefer, S. Mayer, P. Zarda, and H. Weinfurter, Phys. Rev. Lett. **85**, 290 (2000).
[10] D. Press, S. Gotzinger, S. Reitzenstein, C. Hofmann, A. Loffler, M. Kamp, A. Forchel, and Y. Yamamoto, Phys. Rev. Lett. **98**, 117402 (2007).
[11] W. Schmunk, M. Gramegna, G. Brida, I. P. Degiovanni, M. Genovese, H. Hofer, S. Kück, L. Lolli, M. G. A. Paris, S. Peters, M. Rajteri, A. M. Racu, A. Ruschhaupt, E. Taralli, and P. Traina, Metrologia **49**, S156 (2012).
[12] A. Kuzmich, W. P. Bowen, A. D. Boozer, A. Boca, C. W. Chou, L.-M. Duan, and H. J. Kimble, Nature (London) **423**, 731 (2003).
[13] M. Scholz, L. Koch, and O. Benson, Phys. Rev. Lett. **102**, 063603 (2009).
[14] E. A. Goldschmidt, M. D. Eisaman, J. Fan, S. V. Polyakov, and A. Migdall, Phys. Rev. A **78**, 013844 (2008).
[15] M. Aßmann, F. Veit, M. Bayer, M. van der Poel, and J. M. Hvam, Science **325**, 297 (2009).

[16] M. Hennrich, A. Kuhn, and G. Rempe, Phys. Rev. Lett. **94**, 053604 (2005).
[17] D. Elvira, X. Hachair, V. B. Verma, R. Braive, G. Beaudoin, I. Robert-Philip, I. Sagnes, B. Baek, S. W. Nam, E. A. Dauler, I. Abram, M. J. Stevens, and A. Beveratos, Phys. Rev. A **84**, 061802 (2011).
[18] M. Aßmann, F. Veit, M. Bayer, C. Gies, F. Jahnke, S. Reitzenstein, S. Höfling, L. Worschech, and A. Forchel, Phys. Rev. B **81**, 165314 (2010).
[19] J. S. Lundeen, A. Feito, H. Coldenstrodt-Ronge, K. L. Pregnell, C. Silberhorn, T. C. Ralph, J. Eisert, M. B. Plenio, and I. A. Walmsley, Nature Phys. **5**, 27 (2009).
[20] A. E. Lita, A. J. Miller, and S. W. Nam, Opt. Express **16**, 3032 (2008).
[21] G. Brida, L. Ciavarella, I. P. Degiovanni, M. Genovese, L. Lolli, M. G. Mingolla, F. Piacentini, M. Rajteri, E. Taralli, and M. G. A. Paris, New J. Phys. **14**, 085001 (2012).
[22] M. Avenhaus, K. Laiho, M. V. Chekhova, and C. Silberhorn, Phys. Rev. Lett. **104**, 063602 (2010).
[23] D. A. Kalashnikov, S. H. Tan, M. V. Chekhova, and L. A. Krivitsky, Opt. Express **19**, 9352 (2011).
[24] J. F. Dynes, Z. L. Yuan, A. W. Sharpe, O. Thomas, and A. J. Shields, Opt. Express **19**, 13268 (2011).
[25] L. Mandel and E. Wolf, *Optical Coherence and Quantum Optics* (Cambridge University Press, Cambridge, UK, 1995).
[26] F. T. Arecchi, Phys. Rev. Lett. **15**, 912 (1965).
[27] J. H. Churnside, J. Opt. Soc. Am. **72**, 1464 (1982).
[28] G. Brida, I. P. Degiovanni, M. Genovese, A. Migdall, F. Piacentini, S. V. Polyakov, and I. Ruo Berchera, Opt. Express **19**, 1484 (2011).
[29] G. Brida, L. Ciavarella, I. P. Degiovanni, M. Genovese, A. Migdall, M. G. Mingolla, M. G. A. Paris, F. Piacentini, and S. V. Polyakov, Phys. Rev. Lett. **108**, 253601 (2012).
[30] P. R. Tapster and J. G. Rarity, J. Mod. Opt. **45**, 595 (1998).
[31] G. Zambra, A. Andreoni, M. Bondani, M. Gramegna, M. Genovese, G. Brida, A. Rossi, and M. G. A. Paris, Phys. Rev. Lett. **95**, 063602 (2005).
[32] W. P. Grice, A. B. URen, and I. A. Walmsley, Phys. Rev. A **64**, 063815 (2001).
[33] S. S. Straupe, D. P. Ivanov, A. A. Kalinkin, I. B. Bobrov, and S. P. Kulik, Phys. Rev. A **83**, 060302 (2011).